Earthquake Engineering, Tenth World Conference © 1992 Balkema, Rotterdam. ISBN 90 5410 060 5

Estimation of effects of subsurface structure on ground motions using 3-D array data

T. Iwata & K. Irikura
DPRI, Kyoto University, Japan
J.-C. Gariel
DPEI/SERGD, France

ABSTRACT: Vertical-array seismograms obtained from 0m to about 1km in depth are compared with the synthetics computed by the full-wave theory for multi-layered structure model with a deterministic source. The target earthquake ground motions are obtained from a magnitude 6.6 earthquake that occurred 70km east of the site at a focal depth of 44km. At the deepest point in the bed rock, there is a good agreement between the observed and the synthetics. At shallower points, the direct S-wave portions of the synthetics are good agreement with those of the observed, but the later phases of synthetics are poorer than those of observed. These reasons are to be sought in difficulty of adequate modeling near- surface structure. The arrival direction and apparent velocity of the later phases estimated from a surface array data show that these later phases are mainly composed of surface waves which do not always come from the source direction directly. Those later phases can be regarded as secondary generated waves by the edge of sedimentary basins. These result shows that the most required information to predict ground motions faithfully is the surface geological condition. We should evaluate not only reverberation effects of vertical heterogeneity of P- and S-wave velocity and density structures but scattering properties due to horizontal heterogeneity of underground structures, especially near-surface geology including topography.

1. Introduction

It is one of the most important subjects for seismic hazard mitigation to predict strong ground motions. For this purpose, source, propagation-path, and site effects should be considered in model simulations and most important parameters that mainly control the characteristics of ground motions have to be evaluated correctly. To elucidate these effects, one of the direct technique is to compare observed seismograms with waveform synthetics based on a reasonable underground structure and source model.

In this study, we simulate synthetic seismograms by full-wave theory by a multi-layered structure with a deterministic source and compare the synthetics with observed seismogram obtained from the vertical strong-motion array. From this comparison, we discuss about the applicability of the source and underground structure model used here and what information is more required for predicting strong ground motions faithfully.

2. Data

Strong motion records analyzed here were obtained with the vertical and horizontal arrays located at Tomioka (TMK= 140.59E, 37.20N, +50m), Fukushima Prefecture, Japan. At this site, the thickness of tertiary sedimentary layers is about 900 meters. The main station consists of 6 points located at GL-950, -660, -251, -100, -6, 0m, respectively, to form a vertical array. Each point has three-component accelerometer. The deepest observation point is installed in the bed rock with a S-wave velocity of 2.80km/s. In addition to the vertical two sub-stations are installed to form a horizontal triangle array of which apertures are about 150m. The three-component seismometer at each station are set up at GL-6m and -4m, respectively. The profile of velocity, density, and attenuation coefficients were available from well-loggings and refraction surveys with north-south line across this site (Omote et al.,1984). Fig.1(a) shows a detailed underground structure at TMK from the P- and S-wave logging, and formation density logging. In Fig.1(b), we show the underground P-wave velocity structure along the refraction survey line across TMK. From these results, the subsurface structure can be approximated by a multi-layered model. We computed full-wave synthetic seismograms using a model of multi-layered half-space containing a point dislocation source by the Discrete Wavenumber method (Bouchon,1981).

We simulate ground motions from the magnitude 6.6 earthquake that occurred on the 7th of April, 1987, 70km east of the TMK site with focal depth 44km determined by JMA(1987). In Fig.2(a) we show a map of Station TMK and the epicenter of this event together with recent seismic activity near the event. Fig.2(b) shows the focal plane solution of this event with an equal-area projection of lower hemisphere determined by Tohoku Univ.(Faculty of Science, Tohoku Univ., 1987). In Fig.3, we show horizontal acceleration seismograms observed at the deepest point(GL-950m), the integrated velocity seismograms, the Fourier acceleration and velocity amplitude spectra of these records. These records are observed by a digital recording system with a sampling rate of 0.005s. From the acceleration amplitude spectra, we find these records have a sufficient S/N ratio to analyze in the frequency range higher than 0.15Hz. The trough around 0.3-0.4Hz of the NS- component amplitude spectrum is caused by the destructive interference between incident wave from below and reflected wave from the surface. In Fig. 4, we show velocity seismograms of NS- component observed at 6 different-depth points. The velocity seismograms are obtained from the integration of Band-Pass- Filtered (0.2-5.0Hz) acceleration seismograms. In this frequency range, the velocity seismogram observed at the -6m point is almost the same as that at the 0m point. In Fig.4, the direct S wave propagates upward from the deepest point to the surface, and the reflection wave goes down from the surface. The later phases seen after the direct S-waves appear to be clearly "in-phase" between three shallower points(-251, -100, and 0m).

This suggests that these later phases consist of some surface waves propagating horizontally.

3. Simulation of Vertical Array records

First of all, we determine an underground structure model for the simulation. The P- and S-wave velocity and density structure down to a depth of about 1km are determined from the well-logging data as shown in Fig.1. The elastic parameters of deeper structure are determined from a longer-distance refraction survey performed in 1959 along a survey line passing through near Station TMK (The Research Group of Explosion Seismology, 1959). The refraction survey results are shown in Fig. 5. Fig.5(a) shows the map of the refraction survey line together with the position of Station TMK, and Fig.5(b) shows the P-wave velocity structure obtained from this survey. S-wave velocity structure below a depth of 1km is estimated from the P-wave velocity structure assuming a Poison's ratio of 1/4. The depth variation of Q-factor down to 1km was determined by Shima et al.(1984) using seismic records in this vertical array. The density of deeper structure is assumed from empirical relation between the P-wave velocity and the density (Grant and West, 1965). The Q-factor of deeper structure is obtained by Umino and Hasegawa (1984) using micro-earthquake data. The Q-factor is assumed to be constant in each layer and independent on frequency. The assumed parameters of underground structure for the simulation are shown in Fig.6 and listed in Table 1.

For the source model, we assumed a point dislocation source. The fault parameters of dip, strike, and rake angles are determined from P-wave first motions by the Tohoku Univ.(Faculty of Science, Tohoku Univ.,1987), and the source time function is assumed to be a time derivatives of $1/2(1+tanh(t/t_0))$, where t0 is (half) rise time (Bouchon,1981). The rise time t_0 is assumed to be 5s from the empirical relation between the rise time and the magnitude (Sato,1989). The seismic moment of this event is determined from matching the observed amplitude of the direct S- wave portion with the synthetic one at the deepest point (GL- 950m) in the bed rock. The seismic moment obtained here fits the empirical relation between the seismic moment and the magnitude (Sato,1989).

In Fig.7, we show the simulated velocity seismograms (thin line) of NS-component (a) and EW-component (b) together with the observed seismograms (thick line). The simulated velocity at the deepest point agrees very well with the observed one from the direct S-wave portions and later phases both in NS- and EW- components. Also, the simulated velocity of the direct S-wave portions at the shallower points agree well with the observed one, however, the later phases of the synthesis at these observation points can not explain the observation. Simulated velocities at the shallower points have relatively shorter duration than the observations. On the other hand, the observed velocities have longer duration. This different results from that the underground structure shallower than 200m can not be modeled correctly. More complicated underground structure near surface such as, irregular topography, horizontal discontinuity etc., may generate so-called secondary waves and contaminate seismic motions directly coming from the source. Unfortunately, such complex structures are "unmodeled" in this simulation.

4. Analysis of the Surface Array records and Discussion

As mentioned above, three observation points near the surface (at a depth of either -6m or -4m) are installed to form a horizontal triangle array whose aperture is about 150m at Station TMK. In this section, using records at those 3 points, we determine the arrival direction and apparent velocity of direct S-wave portion and later phase portions. Apparent vector velocity with respect to each phase is estimated from the differences of arrival times calculated from the cross correlation between band- pass-filtered seismograms at each two points. To calculate the correlation, the time window with the Hanning's shape is taken to be three times longer than the center period of each band-pass- filter.

In Fig. 8, we show apparent vector velocity diagram together with the vertical-component seismograms at 3 points of the horizontal array. From top to bottom, the diagrams show the inverse of apparent velocity, i.e. slowness, in the direction of wave propagation with the center frequency from 0.25 to 1.25Hz at intervals of 0.25Hz and from left to right, those of the center time of the window from S-wave onset to 10seconds later at intervals of 1.0s. From this figure, the direct S-wave portions comes from the east with an apparent velocity of 4-5km/s. This means that the direct S-wave propagates almost vertically. On the other hand, the later phases, being 3s later from the S-wave onset and 5s later, propagate from the north to the south direction and from the west to the east direction, respectively, with an apparent velocity of 0.5-2km/s. These later phases arrive differently from the source direction. Moreover, these later phases propagate nearly horizontally in consideration of the relatively small apparent velocities.

The reasons why we can not explain these later phases in our simulations are as follows. The simulation can not contain the scattering and the multi-path waves because of assuming a horizontally stratified multi-layered structure model with a point source. From the observation records in the vertical array in the section 2, we pointed out later phases around 5s after from the S-wave onset are "in-phase" between shallower observation points. These phases consist of the surface wave arriving from the west direction different from the source. Probably, these surface waves that propagate horizontally inside the basin are generated by the finiteness of surface layers at the edge of the basin in the case of body wave incidence . Actually, there is a hilly zones 2-3km east away from Station TMK as shown in Fig.9. Therefore, those basin-induced surface waves arriving around 5s after the S-wave onset might be generated at the interface between sedimentary basin and hilly zones.

5. Conclusions

Vertical array seismograms ranging from 0m to 950m in depth are compared with the synthetics computed using the full-wave theory for a multi-layered structure model with a deterministic source. The target earthquake ground motions are obtained for a magnitude 6.6 earthquake that occurred 70km east of the site at a focal depth of 44km. The synthetic seismograms of horizontal NS and EW components at the deepest point of GL-950m in the bedrock are in a good agreement with those of the observed ones. At the shallower points of Gl-250m, -100m, and 0m in the Tertiary sediments, the direct S-wave portions of the synthetic seismograms are in a good agreement with those of the synthetic ones, however the later phases of the synthetic ones are poorer than those of the observed ones. These reasons are to be sought in difficulty of adequate modeling near surface structure. We assume only vertical heterogeneity but not horizontal heterogeneity.

To make it clear why the later phases at the shallow points can not be explained by the simulation, we examined the wave types of such phases using the surface tripartite array data. The results show that these later phases are mainly composed of surface waves which are not always come from the source direction directly. Those later phases can be regarded as secondary generated waves by irregular subsurface structures such as the edge of sedimentary basins. To elucidate the effects of local site conditions on wave propagation, we should know

not only vertical heterogeneity of P- and S-wave velocity and density structures but horizontal heterogeneity of underground structures, especially near the surface.

acknowledgments

Vertical array data at TMK are presented by the Research Committee on Earthquake Observation with Vertical Instrument Array in Rock jointly founded by ten electric power companies in Japan.

References

Bouchon, M. 1981. A simple method to calculate Green's function for elastic layered media. *Bull. Seismol. Soc. Am.* 71 : 959-971.

Faculty of Science, Tohoku University. 1987. Microearthquake activity in and around the Tohoku distinct (Nov.,1986 - Apr.,1987). *Report on the Coordinating Committee for Earthquake Prediction* 38 : 11-44.

Grant, F.S. and G.F. West. 1965. *Interpretation theory in applied geophysics.* McGraw-Hill Co. LTD.

JMA. 1987. Seismic activity in the region off Fukushima prefecture (Feb. - Apr., 1987). *Report on the Coordinating Committee for Earthquake Prediction* 38 : 53-63.

Omote, S., Y. Osawa, B. Ohmura, S. Iizuka, T. Ohta, and K. Takahashi. 1984. Observation of earthquake strong-motion with deep boreholes - An introductory notes for Iwaki and Tomioka observation station in Japan -. *Proc. 8th World Conf. of Earthq. Eng.*

The Research Group of Explosion Seismology. 1959. Observations of seismic waves from the second Hokota explosion. *Bull. Earthq. Res. Inst., Univ. of Tokyo.* 37 : 495-508.

Shima, E., T. Ohta, S. Iizuka, K. Takahashi, H. Ishida, and F. Matsueda. 1984. A study on characteristics of seismic motions in the rock with vertical instrument arrays, part 5: Evaluation of damping factor using direct S-wave in the rock. *Proc. Art. Eng. of Japan* : 2018.

Sato, Y. 1989. *Handbook of Seismic Fault Parameters in Japan.* Kajima Pub. Co. Ltd.

Umino, N. and A. Hasegawa. 1984. Three-dimensional Qs structure in the northeastern Japan arc. *Jour. Seismol. Soc. Japan* 37 : 217- 228.

Table 1 Parameters of the structure model for simulations.

Depth (m)	Vp (m/s)	Vs (m/s)	Den. (g/cm^3)	Qp	Qs
92.	1800.	520.	1600.	40.	20.
120.	1800.	700.	1650.	45.	22.
476.	2100.	930.	1800.	50.	25.
580.	2500.	1200.	1720.	60.	30.
630.	2500.	1250.	1720.	80.	40.
792.	2800.	1350.	2200.	100.	50.
810.	2800.	1200.	2000.	100.	50.
820.	3200.	1400.	2000.	120.	60.
847.	4300.	2100.	2400.	200.	100.
896.	4600.	2300.	2470.	300.	150.
910.	4400.	2200.	2470.	300.	150.
5000.	5500.	2800.	2600.	500.	300.
22000.	6200.	3590.	2800.	900.	450.
	7700.	4450.	3100.	1000.	500.

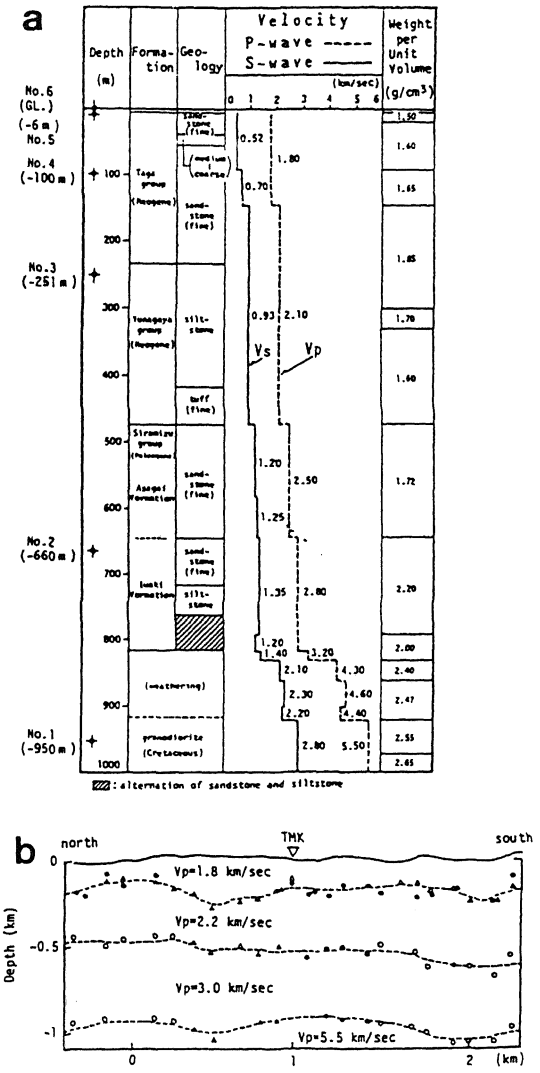

Fig.1 (a) Underground structure along the Tomioka (TMK) vertical array and observation points. (b) Subsurface P-wave velocity structures near Station TMK. The refraction survey was carried out across Station TMK (after Omote et al.,1984).

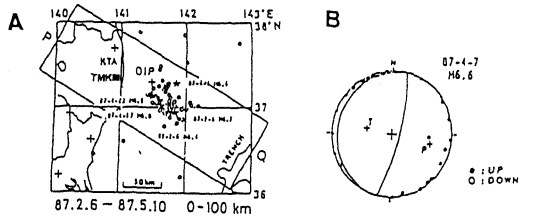

Fig.2 (a) Map of Station TMK and the epicenter of the event at 7th April, 1987 with MJMA=6.6. (b) Fault plane solution of the event. Projection is the equal-area projection of lower hemisphere (after Tohoku Univ.,1987).

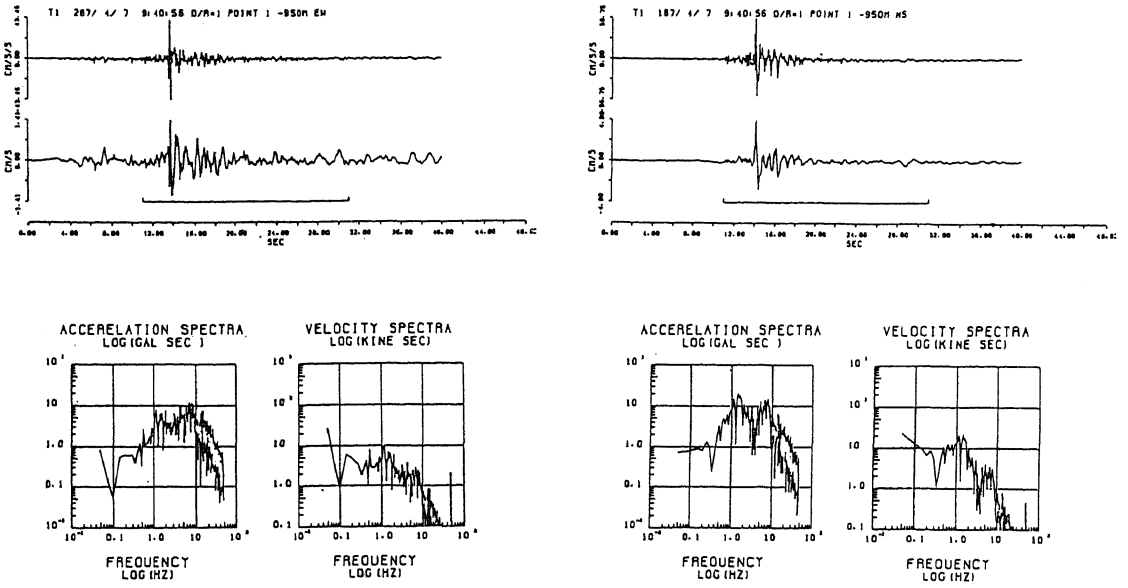

Fig.3 Observed acceleration seismograms, the integrated velocity seismograms, and the spectra of NS and EW components at GL -950m observation point. Left hand side shows the EW component and the right, the NS component.

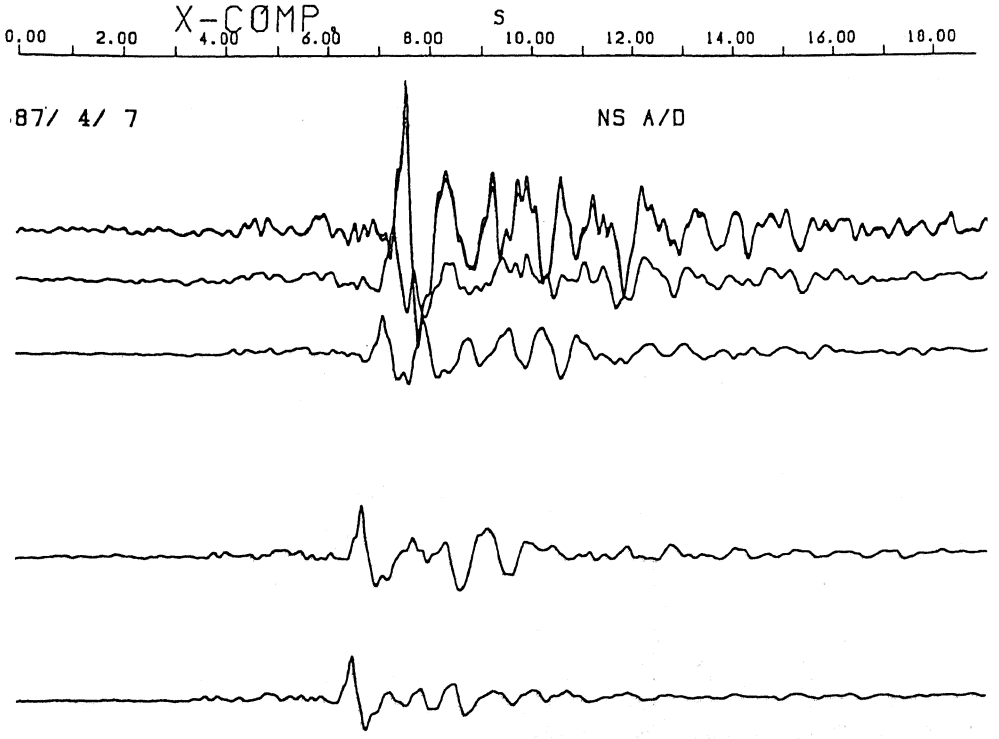

Fig.4 Integrated velocity seismograms of NS-component observed at five points with different depths (-950, -660, -251, -100, and 0m).

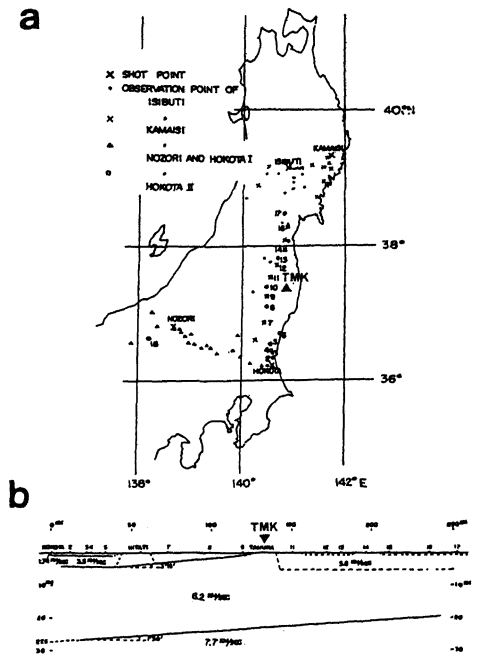

Fig.5 (a) Shot (cross) and observation (open circle) points of the refraction survey. (b) Obtained P-wave velocity structure model (after the Research Group for Explosion Seismology, 1959).

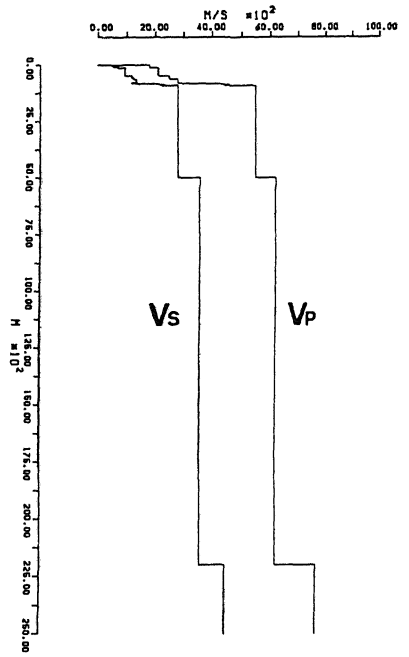

Fig. 6 Underground structure model for simulation.

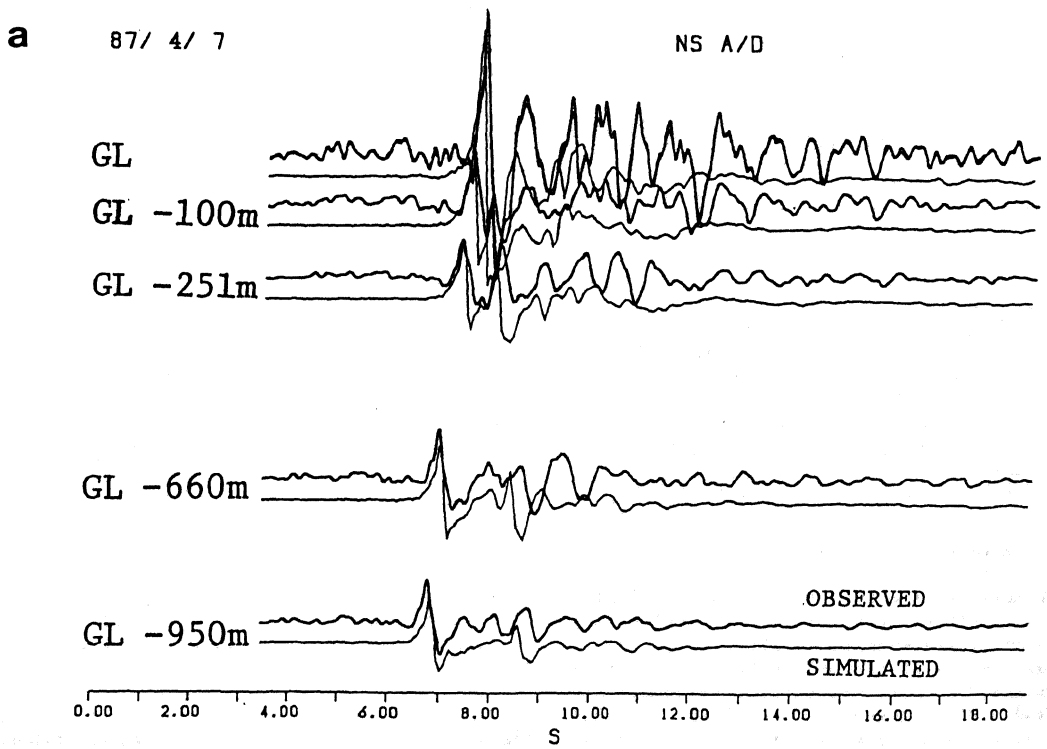

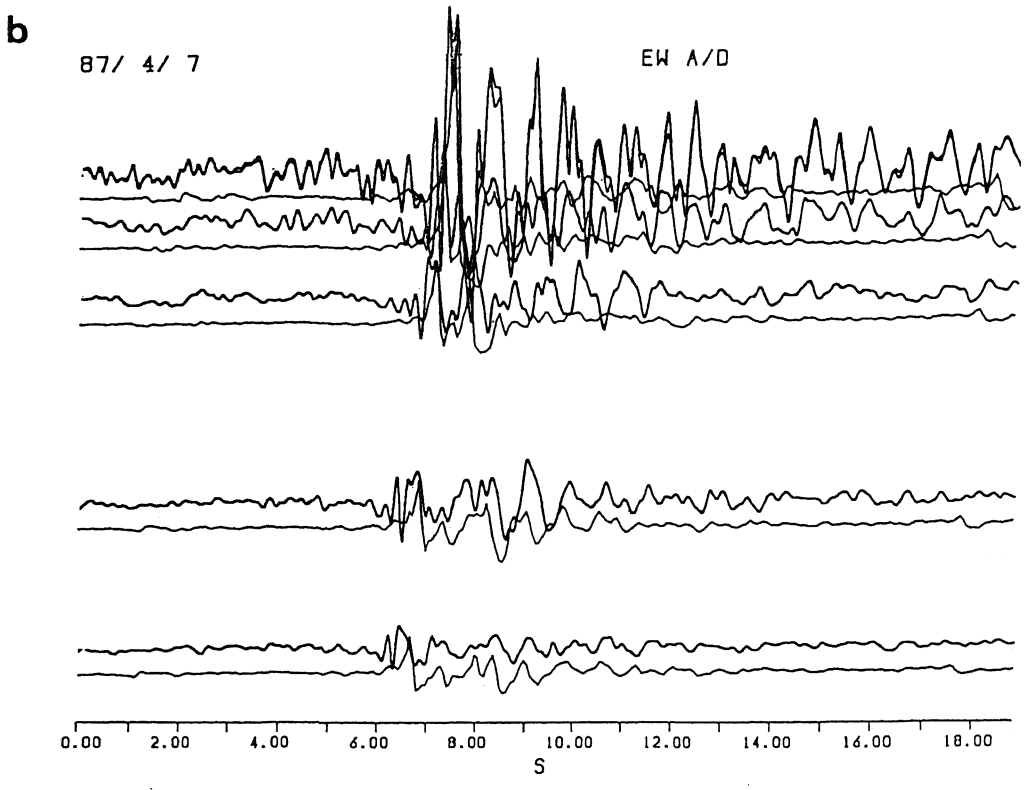

Fig.7 Simulated and observed velocity seismograms of EW and NS components. Thin lines show the simulation and thick lines, observation. (a) shows the NS component and (B) the EW component.

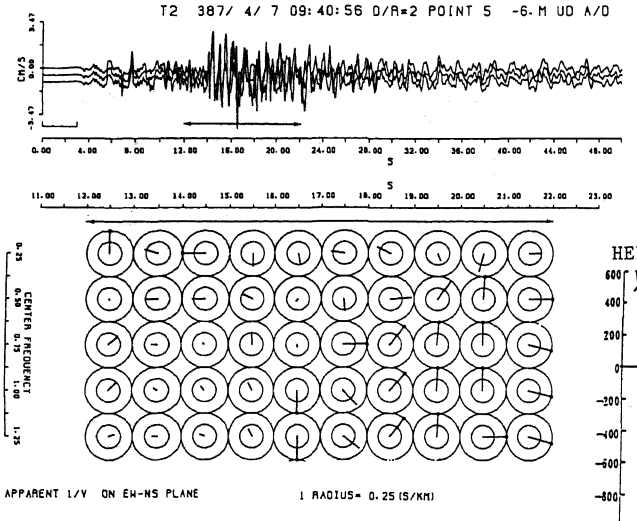

Fig.8 Apparent vector velocity diagram together with the vertical-component seismograms at 3 points of the horizontal array. From top to bottom, the diagrams show the inverse of apparent velocity, i.e. slowness, in the direction of wave propagation with the center frequency from 0.25 to 1.25Hz at intervals of 0.25Hz and from left to right, those of the center time of the window from S-wave onset to 10seconds later at intervals of 1.0s.

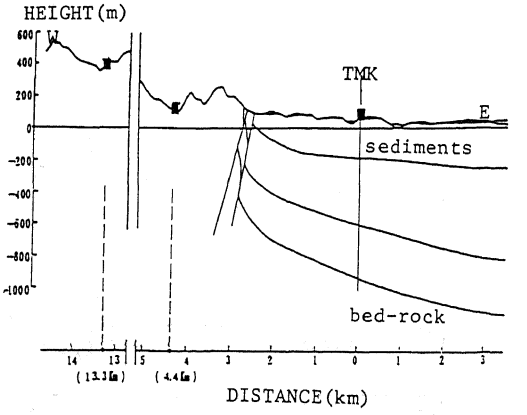

Fig. 9 Vertical cross section of assumed geological structures along the east-west line passing through Station TMK.